RSC Advances

ROYAL SOCIETY OF CHEMISTRY

www.rsc.org/advances

RSC Advances

Cite this: DOI: 10.1039/c0xx00000x

www.rsc.org/xxxxxx

COMMUNICATION

The stereochemistry of two monoterpenoid diastereomers from *Ferula dissecta*†

Zhi-Qiang Wang,[a] Chao Huang,[a] Jian Huang,*[a] Hong-Ying Han,[b] Guo-Yu Li,[b] Jin-Hui Wang,[a] and Tie-Min Sun*[a]

Received (in XXX, XXX) Xth XXXXXXXXX 20XX, Accepted Xth XXXXXXXXX 20XX
DOI: 10.1039/b000000x

Two diastereomeric monoterpene benzoates, tschimganin and *iso*-tschimganin, were isolated from the roots of *Ferula dissecta*. The absolute stereochemistry of the compounds was determined by chemical-related methods and *ab initio* calculations of electronic circular dichroism and ^{13}C-NMR shifts. The antitumor activities of the diastereomers were also tested.

Ferula, flowering plants from the family Apiaceae, is native to the Mediterranean region east of central Asia and mostly grows in arid climates. *Ferula* presents interesting phytochemical features, such as the occurrence of sesquiterpenes[1-3] and sesquiterpene coumarins.[4-7]As one of the species of Ferula, *Ferula dissecta* (Ledeb.) Ledeb is distributed mainly in northwest China, such as in Xinjiang, [8] and has a long history of application in the treatment of digestive diseases and arthritis in Uygur medicine.[9] During our search for structurally unique and biologically interesting natural products, [10] two diastereomeric monoterpene benzoates (**1** and **2**; Fig. 1) were isolated from the roots of *F. dissecta* collected in Xingjiang, China. Compound **1** was identified as tschimganin by comparison of its spectroscopic data with the literature values, which had previously been isolated from some *Ferula* species and propolis in Iran and Russia with estrogen-like activity, significant cytoxicity against the MCF-7, HepG2, and MDBK cell lines, [11, 12] and considerable antimicrobial activities against *S. aureus*[13]. And compound **2** was identified as the diastereomers of tschimganin, *iso*-tschimganin. Although these compounds have been reported in previous literatures, [11-14] their stereochemistry, especially absolute configuration (AC), has not yet been investigated.

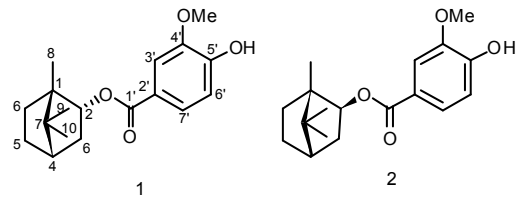

1 2

Fig.1 Chemical structures of **1** and **2**

In this paper, the chemical structures of **1** and **2** as well as their ACs were elucidated by extensive spectroscopic methods, electronic circular dichroism (ECD), and theoretical calculations. Correlations between cotton effects (CEs) and molecular structures were evaluated. Configurational assignments were further confirmed by comparison of the experimental and calculated NMR data. In addition, the experimental ECD curves of **1** and **2** were compared with those of two structural analogs, which were synthesized from commercially available chiral precursors with definite ACs. Finally, the antitumor activities of **1** and **2** were evaluated.

The roots of *F. dissecta* were collected in Tuoli, Xinjiang, China in June 2007 and identified by Dr. Yong Tan (Shihezi University of China). A voucher specimen (No. 20071018001) was deposited in School of Pharmacy, Shihezi University.

Air-dried roots (1.45 kg) of *F. dissecta* were extracted three times by 95% ethanol after refluxing for 3 h. The combined solutions were concentrated under vacuum to yield an extraction of 240 g. Part of the ethanol extract was subjected to column chromatography over silica gel and eluted with petroleum ether (PE) with increasing amounts of EtOAc to afford Fr. A (PE-EtOAc, 100:0.5, 0.7 g) and Fr. B (PE-EtOAc, 100:1.5, 0.5 g). Fr. A was then separated by HPLC (H_2O-AcCN, 55:45) to produce compound **1** (20.0 mg, 126.2 min). Fr. B was also subjected to HPLC (H_2O-AcCN, 55:45) to produce compound **2** (2, 37.0 mg, 119.2 min).

Compound **1** was isolated as white grease, easily dissolved in chloroform and ethyl acetate. Its IR spectrum indicated the presence of hydroxyl and carbonyl groups at 3437 and 1677 cm^{-1}, respectively. A molecular formula of $C_{18}H_{24}O_4$ was determined by HR-ESI-MS at m/z 305.1750 $[M+H]^+$ (calcd.$C_{18}H_{25}O_4$, 305.1753). The ^{1}H-NMR (300 MHz, $CDCl_3$) spectrum of compound **1** showed three aromatic proton signals in an ABX system at δ_H 7.64 (1H, dd, J = 8.4, 1.8 Hz, H-7′), 7.60 (1H, d, J = 1.8 Hz, H-3′), and 6.96 (1H, d, J = 8.4 Hz, H-6′), which were assigned to one 1,3,4-trisubstituted benzene ring, one methoxyl proton at δ_H 3.95 (3H, s), and three methyl protons of each 3H singlets at δ_H 0.97, 0.92, and 0.91, respectively. The fact that one ester carbonyl group was connected to the phenyl group was

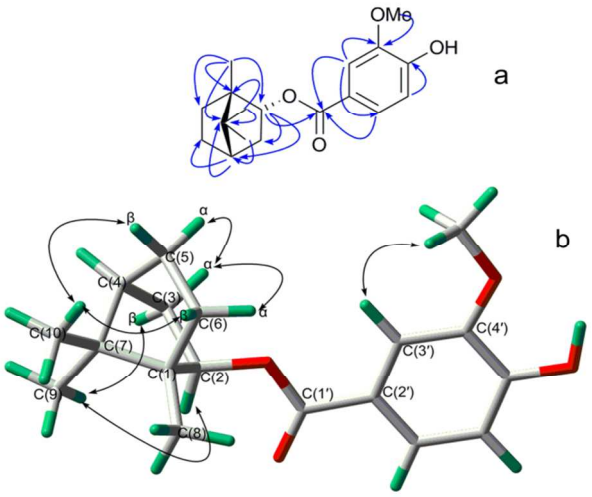

Fig. 2 The key HMBC (a) and NOESY (b) correlations of **1**

supported by the resonance at δ_C 166.6 in the ^{13}C-NMR (75 MHz, $CDCl_3$) spectrum and the absorption peak in the IR spectrum at 1677 cm^{-1}, which indicated a conjugated nature. Except for one methoxyl carbon signal at δ 56.1 and seven 3,4-disubstituted benzoyl skeleton signals, ten carbon resonances ascribable to a bornane monoterpene moiety were detected. The methoxyl group at C-4′ was confirmed by HMBC correlations between δ_H 3.95 and δ_C 146.2. Correlation of the proton signal at δ_H 5.08 with the carbonyl carbon at δ_C 166.6 indicated the location of a benzoyloxy group at C-2. NOESY cross-peaks between H-2 and Me-9 suggested that H-2 and Me-9 were cofacial on the same side of the ring (Fig. 2). Based on the aforementioned analysis and comparison of the spectroscopic data with literature values, [12]compound **1** was identified as tschimganin.

Compound **2** was also obtained as white grease, also easily dissolved in chloroform and ethyl acetate. Its IR spectrum indicated the presence of hydroxyl and carbonyl groups at 3366 and 1691 cm^{-1}. The molecular formula of compound **2**, $C_{18}H_{24}O_4$, was determined by pseudo-molecular ion peaks at *m/z* 609.3423 $[2M+H]^+$ (calcd.$C_{36}H_{49}O_8$, 609.3427) in the ESI-TOF-MS. The ^{1}H-NMR (300 MHz, $CDCl_3$) spectrum of compound **2** also showed three aromatic proton signals in an ABX system at δ_H 7.59 (1H, br d, J = 8.4Hz, H-7′), 7.55 (1H, br s, H-3′), and 6.93 (1H, d, J = 8.4Hz, H-6′), one methoxyl proton at δ_H 3.93 (3H, s), and three methyl protons at δ_H 1.12, 0.91, and 0.88, respectively.

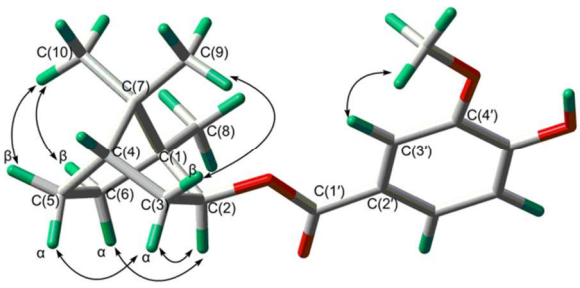

Fig.3 The key NOESY correlations of **2**

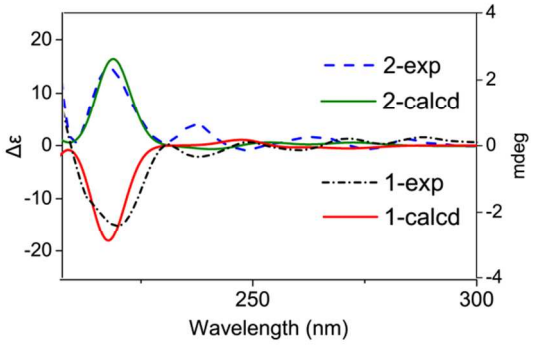

Fig.4 Experimental and calculated ECDs of **1** and **2**

Its ^{13}C-NMR (75 MHz, $CDCl_3$) spectrum showed one methoxyl carbon signal at δ_C 56.1, seven 3,4-disubstituted benzoyl skeleton signals, and ten carbon resonances ascribable to a bornane monoterpene moiety. Considering its molecular formula, compound **2** was determined to feature the same planar structure as **1**. Fig.3 shows the key NOESY correlations of 2 which suggested that H-2 and Me-9 presented a *trans* relationship (The detailed NOESY experiments of **1** and **2** are shown in Fig.S7 and Fig.S16, respectively). Thus, compound **2** was identified as *iso*-tschimganin.

The stereochemistry assignments of **1** and **2** were determined by ECD and quantum chemical calculations. The experimental ECD of **1** recorded in MeOH (4.86×10^{-4} M) in the 200–300 nm range showed a remarkably negative CE at 218 nm and a weakly negative CE at 232 nm (Fig.4). The ECD of **2** showed, as expected, a perfect mirror image of **1**, two positive CEs at 218 and 232 nm. The ECDs of the two isomers were simulated in the program package Gaussian 09. [15] First, conformational searches were performed with the MMFF94 force field by arbitrarily fixing the absolute configuration of C-2 for compounds **1** and **2**. Twelve possible conformers of **1** and **2** were found, respectively, and these were fully optimized in methanol at the DFT/B3LYP/TZVP (PCM) level of theory. Three stable low-energy conformations of **1** and **2** were obtained, respectively (shown below). The rotations of single bonds connecting the bornane monoterpene moiety and substituted phenyl ring led to the conformational change.

Moreover, the ECD spectra of stable conformers were calculated based on the time-dependent density functional theory (TDDFT) method at the CAM-B3LYP/TZVP level.[16, 17]The final ECD curves were generated using Boltzmann weighting. Figure 4 shows the calculated ECDs of **1** and **2** after UV correction of 13 nm. The calculated ECD of **1** showed strong negative CE at 218 nm, similar to that in the experimental spectrum of **1**, and the simulated ECD of **2** perfectly mirrored that of **1**, again similar to the experiment of **2**. Notwithstanding the discrepancy between the calculated and experimental ECD in other spectral ranges, this result supports the assignments of a (1*S*, 2*R*, 4*S*) AC to **1** and a (1*S*, 2*S*, 4*S*) AC to **2**. In order to get reliable results, TD-DFT/CAM-B3LYP/aug-cc-pVDZ ECD calculations were also performed for the conformers on DFT/B3LYP/cc-pVDZ input geometries. The calculation model implemented in geometry

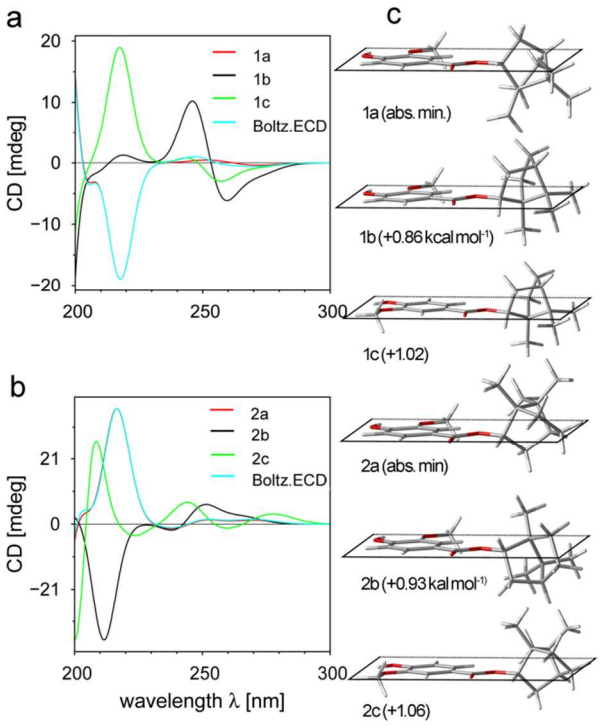

Fig. 5 The relative stable conformers of **1** and **2**, and their calculated ECDs. The ECDs of conformers **1a** and **2a** (red lines) are covered by the Boltzmann-averaged curves (cyan lines).

optimization provided a new conformer distribution (Table S3), yet the Boltzmann-weighted ECD retained the band shapes, showing only a small blue shift (Fig.S23a, Fig.S23b). Also the use of different functionals and basis sets in the calculations did not lead to appreciable changes in the ECD curve profile of individual conformers (Fig.S23c).

The origin of the CEs at 218 nm in the experimental ECDs of **1** and **2** could be explained by molecular orbital (MO) analysis at the same level of ECD calculation (Fig. S24). As inferred from the MO analysis, the CE at 218 nm is mainly dominated by transitions from HOMO-1→LUMO (47%) and HOMO→LUMO (51%), which could be ascribed to the combination of a phenyl ring π→π* transition and a carbonyl group *n*→π* transition.

In our studies of the relationship between the stereostructures and the CEs, some interesting phenomena were observed and valuable results were obtained. As demonstrated earlier, the Boltzmann-averaged calculated ECD of **1** is a perfect mirror image of **2**, similar to the experimental findings. However, the calculated ECDs of individual conformers vary greatly because of conformational changes brought about by rotations of single bonds. Figure 5 shows the stereostructures of the stable conformers and their calculated ECD spectra. By viewing the conformers along the O–C direction of the carbonyl group, a plane passing through the phenyl ring and the carbonyl group can divide the borneol moiety into two parts. An obvious positive relevance exists between the CE at 218 nm and the upper part of the borneol moiety. The larger part (three methyl groups, a methylene group, and a methylidyne group) of the borneol moiety is located in a lower region in conformer **1a**; thus, the calculated ECD displays a negative CE at 218 nm. In contrast to **1a**, the upper parts (three methylene groups and a methylidyne group) are larger than the lower parts (only two methyl groups) in the **1b** and **1c** structures; therefore, positive CEs are observed. The difference in magnitude between **1b** and **1c** may be due to the methoxy group, which dominates the *n*→π* transition from the oxygen atom to the phenyl ring. As **1a** is the preferred conformation in methanol, occupying the highest Boltzmann population (80%; Table S3) among the conformers, the weighted ECD shows a negative CE at 218 nm, in agreement with the experimental results.

Similar phenomena may be observed in compound **2** (Fig. 5b). The positive CEs in **2a** and **2c** may be attributed to the fact that the larger part of the molecule (three methyl groups, a methylene group and a methylidyne group) are located above the plane, and the negative CE in **2b** is easy to understand in a similar manner. Based on the aforementioned analyses, we presume that any atom or group occupying the space outside the plane may break the symmetry of the molecule and lead to a change in CE. This case is similar to the "octant rule", a well-known semi-empirical approach for predicting the sign of the CE of the *n*–π* transition of saturated ketones. However, the octant rule is usually used for saturated cyclic ketones and is not suitable for open chain esters. Our work provides a useful clue for predicting the sign of the CE of open chain esters.

Interest in the use of *ab initio* prediction of ^{13}C-NMR chemical shifts to aid stereo structural assignment has recently increased. [18, 19]Considering that some differences between the NMR data of **1** and **2** were observed, we attempted to further confirm the stereo

Table.1 Experimental and Calculated ^{13}C-NMR Chemical Shifts δ (ppm) of **1** and **2**

Position	**1**		**2**	
	δ (calc.)[a]	δ (exp.)	δ (calc.)	δ (exp.)
1	54.9	49	53.1	49.1
2	84.4	81.3	83.3	80.3
3	40.7	38.9	38.7	36.9
4	48.7	45.1	46.8	45
5	32.4	27.1	30.2	28.1
6	35.5	33.7	33.2	27.4
7	53.0	47	51.2	47.8
8	10.6	11.6	7.8	13.6
9	18.9	20	16.3	18.9
10	19.6	20.1	17.0	19.7
1′	172.9	165.8	173.9	166.6
2′	128.6	123.1	128.6	123.1
3′	113.9	111.8	113.5	111.7
4′	152.3	146.2	152.8	146.2
5′	159.3	149.8	160.0	149.8
6′	119.1	114.1	118.8	113.9
7′	133.2	123.9	133.3	123.9
4′-CH_3O	54.8	56	53.0	56.1

[a] The theoretical chemical shifts were empirically scaled by using the following equations: $\delta_{scaled} = (\delta_{calc} - intercept)/slope$. Where slope and intercept are obtained from a plot of the calculated data against the experimental data; the purpose of this approach is to remove systematic errors in the shift calculation.

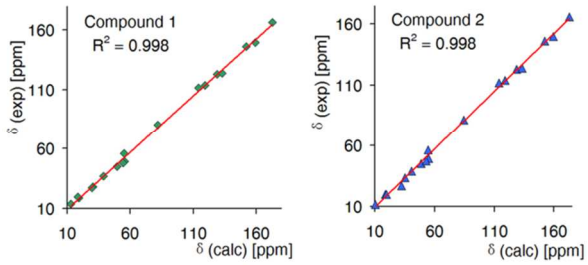

Fig. 6 Correlations of ^{13}C chemical shifts of **1** and **2**

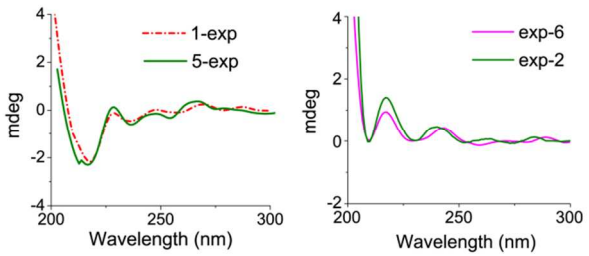

Fig. 7 Comparison of experimental ECDs of **1**, **2, 5**, and **6**

chemistry of the chiral molecules by comparing their theoretical NMR shifts with the available experimental data. NMR shifts for the potential structures were calculated by the GIAO method using the optimized parameters obtained from the B3LYP/6-311++G (d, p) level. Table 1 shows the experimental and Boltzmann-averaged calculated ^{13}C-NMR chemical shifts.

The trends for the ^{13}C-NMR chemical shifts of C-1~C-4, C-9, and C-10 of compounds **1** and **2** were generally well reproduced. However, some noticeable discrepancies for the group (atoms C-1′, C-4′, and C-5′) were evident. This is most probably attributable to the role of the electron correlation associated with the presence of the lone pairs on the oxygen atoms bonded to each of the three carbon atoms C-1′, C-4′, and C-5′. Notwithstanding the discrepancy, the experimental and calculated shifts were in fact highly linearly correlated (Fig. 6). These findings show that the proposed structures match the authentic structures very well.

In our research, we attempted to synthesize **1** and **2** from raw materials with definite configurations but failed because the hydroxyl group attached to the benzene ring was easily oxidized during the synthetic process. Thus, two other stable compounds with closely related structures (1*S*,2*R*,4*S*)-1,7,7-trimethylbi- cyclo [2.2.1]heptan-2-yl-5′-methoxybenzoate (**5**) and (1*S*,2*S*,4*S*)-1,7,7-trimethylbicyclo[2.2.1]heptan-2-yl-5′-methoxybenzoate (**6**) (Scheme 1) were prepared from the commercially available chiral precursors (**3** and **4**). As **3** and **4** show chiral structures similar to those of **1** and **2**, respectively, similar ECD spectral features are expected.

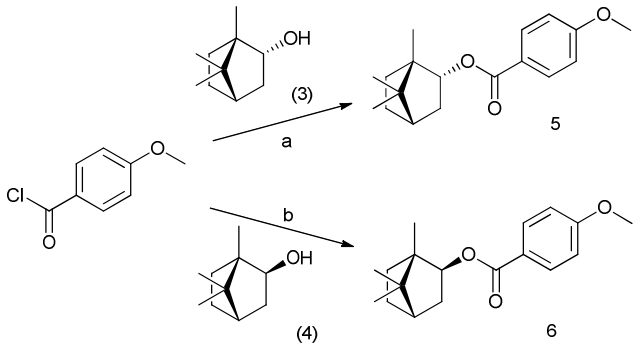

Scheme 1. Reagents and conditions: (a) 1,8-Diazabicyclo[5.4.0]-undec-7-ene (DBU), CH_2Cl_2, 0 °C for 30min before 4-methoxybenzoyl chloride was added, then 0 °C for 1 h, 75.5%; (b) DBU, CH_2Cl_2, 0 °C for 30min before 4-methoxybenzoyl chloride was added, then 0 °C for 1 h, 80.1%.

The synthesis of **5** and **6** is presented in Scheme 1. Compound **5** was synthesized through acylation of the chiral starting material **3** by 4-methoxybenzoyl chloride. The crude product was purified by silica gel chromatography to obtain a white solid compound **5**. Compound **6** was synthesized using **4** as a chiral source via a process similar to that used for synthesizing **5**. Figure 7 shows the ECD curves of **1** and **5**. A strong resemblance between the ECD curves of **1** and **5** may be observed and both compounds exhibit a negative CE at 218 nm. A remarkable similarity between the ECDs of **2** and **6** was also observed over a wide spectral range.

Based on the above evidence, the complete structure of **1** was determined as (1*S*,2*R*,4*S*)-1,7,7-trimethylbicyclo[2.2.1]- heptan-2-yl-5′-hydroxy-4′-methoxyben-zoate and that of **2** was determined as (1*S*, 2*S*, 4*S*)-1,7,7-trimethylbicyclo[2.2.1]heptan-2-yl-5′-hydroxy-4′-methoxyben-zoate.

The growth inhibition effects of **1** and **2** against cervical HeLa cells were investigated. **1** and **2** exhibited different degrees of cytotoxic effects against HeLa cells at 24 h after treatment with IC_{50} values of 32.1 and 29.1 μM, respectively.

In summary, this communication reports the isolation and structural identification of two natural diastereomeric monoterpene benzoates, tschimganin and *iso*-tschimganin. The structures of the diastereomers as well as their ACs were determined by comprehensive spectroscopic data, ECD, and quantum chemical calculations. Configurational assignments were further confirmed by the strong correlation between the experimental and calculated ^{13}C-NMR data and the remarkable similarity of ECDs between the isomers and their synthetic analogs. In addition, a useful reference for predicting the sign of the cotton effect (CE) of open chain esters was provided by analyzing the correlation between the stereostructures of individual conformers and their ECDs. The antitumor activities of the compounds were evaluated and significant growth inhibitory activities against cervical cancer HeLa cells were observed.

Financial support of this research was provided by the Program for Innovative Research Team of the Ministry of Education, Program for Liaoning Innovative Research Team in University, Key Projects of the National Science and Technology Pillar Program (2012BAI30B02), National Natural Science Foundation (U1170302, 81303270) and Shenyang pharmaceutical university scientific research fund (ZCJJ2013407). The theoretical calculations were conducted on the ScGrid and Deepcomp7000 the Supercomputing Center, Computer Network Information Center of Chinese Academy of Sciences.

Notes and references

[a] *Key Laboratory of Structure-Based Drug Design and Discovery, Shenyang Pharmaceutical University, Ministry of Education. Shenyang 110016, PR China. Tel./fax: +86-24-23986398. E-mail: suntiemin@126.com.*

[b] *School of Pharmacy, Shihezi University, Shihezi. 832002, PR China*

† Electronic Supplementary Information (ESI) available: Detailed description of the experimental procedures, a listing of UV, IR, HR-EI-MS, NMR spectra, ECDs, computational details and synthetic process. See DOI: 10.1039/b000000x/

1 G. Appendino, J. Jakupovic, S. Alloatti and M. Ballero. *Phytochemistry*, 1997, **45**, 1639 - 1643.

2 K. Kojima, K. Isaka, O. Purev, G. Jargalsaikhan, D. Suran, H. Mizukami, and Y. Ogihara. *Chem. Pharm. Bull.*, 1999, **47**, 690 - 691.

3 K. Kojima, K. Isaka, P. Ondognii, O. Zevgeegiino, K. Davgiin, H. Mizukami, and Y. Ogihara. *Chem. Pharm. Bull.*, 1999, **47**, 1145 - 1147.

4 R. D. H. Murray. *Nat. Prod. Rep.*, 1989, **6**, 591 - 624.

5 A. A. Ahmed. *Phytochemistry*, 1999, **50**, 109 - 112.

6 B. N.Su, Y. Takaishi, G. Honda, M. Itoh, Y. Takeda, O. K. Kodzhimatov, and O. Ashurmetov. *J. Nat. Prod.*, 2000, **63**, 436 - 440.

7 B. N.Su, Y. Takaishi, G. Honda, M. Itoh, Y. Takeda, O. K. Kodzhimatov, and O. Ashurmetov. *J. Nat. Prod.*, 2000, **63**, 520 - 522.

8 A. G. Gonzalez, and J. B. Barrera. *Progress in the Chemistry of Organic Natural Products*, 1995, **64**, 1 - 92.

9 Jiangsu New Medical College. Dictionary of Chinese traditional drugs. Shanghai: Shanghai Scientific and Technical Publishers, 1988, 1174.

10 J. Huang, H-Y. Han, G-Y. Li, H. Y, W-C. Zhang, K. Zhang, Y. Tan, P-Y Li, and J-H. Wang. *J Asian Nat Prod Res*, 2013, **15**, 1100-1106.

11 S. Sahranavard, F. Naghibi, M. Mosaddegh, S. Esmaeili, P. Sarkhail, M. Taghvaei, and S. Ghafari. *Res Pharm Sci*, 2009, **4**, 133-137.

12 S. S. Nazrullaev, A. I. Saidkhodzhaev, Kh. S. Akhmedkhodzhaeva, V. N. Syrov, B. F. Rasulev, and Z. A. Khushbaktova. *Chem Nat Compd*, 2008, **44**, 572-577.

13 B. Trusheva, I. Todorov, M. Ninova, H. Najdenski, A. Daneshmand, and V. Bankova. *Chem Cent J*, 2010, **4**, 8.

14 K. A. Eshbakova and A. I. Saidkhodzhaev. *Chem Nat Compd*, 2003, **39**, 221-222.

15 Gaussian 09, Revision C.01; Gaussian, Inc.: Wallingford, CT, 2010.

16 G. Giuseppe Mazzeo, E. Santoro, A.Andolfi, A. Cimmino, P. Troselj, A G. Petrovic, S. Superchi, A. Evidente, and N. Berova. *J. Nat. Prod.* 2013, **76**, 588 − 599.

17 A. Evidente, S. Superchi, A. Cimmino, G. Mazzeo, L. Mugnai, D. Rubiales, A. Andolfi and A.-M. Villegas-Fernández. *Eur. J. Org. Chem*. 2011, 5564–5570.

18 S. D. Rychnovsky. *Org. Lett.* 2006, **8**, 2895 - 2898.

19 K. C. Nicolaou and M. O. Frederick. *Angew. Chem. Int. Ed.* 2007, **46**, 5278 - 5282.

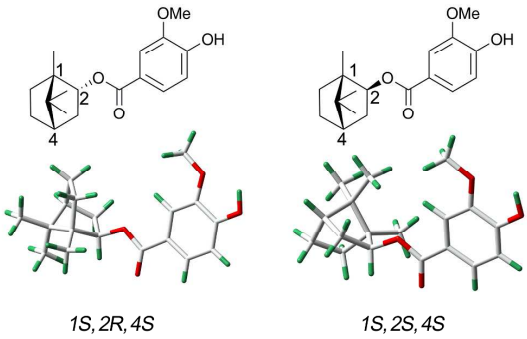

1S, 2R, 4S *1S, 2S, 4S*

The absolute stereochemistry of tschimganin and *iso*-tschimganin was determined by chemical-related methods and *ab initio* calculations of ECD.